

Preparation of magnetic chitosan-supported palladium-5-amino-1*H*-tetrazole complex as a magnetically recyclable catalyst for Suzuki-Miyaura coupling reaction in green media

Mahmoud Nasrollahzadeh^{a,*}, Raziye Bakshali-Dehkordi^a, Taghi A. Kamali^a, Yasin Orooji^{b,*}, Mohammadreza Shokouhimehr^{c,*}

^a Department of Chemistry, Faculty of Science, University of Qom, PO Box 37185-359, Qom, Iran

^b Jiangsu Co-Innovation Center of Efficient Processing and Utilization of Forest Resources, International Innovation Center for Forest Chemicals and Materials, College of Materials Science and Engineering, Nanjing Forestry University, Nanjing 210037, China

^c Department of Materials Science and Engineering, Research Institute of Advanced Materials, Seoul National University, Seoul 08826, Republic of Korea



ARTICLE INFO

Article history:

Received 19 April 2021

Revised 29 May 2021

Accepted 6 June 2021

Available online 12 June 2021

Keywords:

Fe₃O₄ MNPs

Chitosan

5-Amino-1*H*-tetrazole

Palladium complex

Suzuki-Miyaura

Green media

ABSTRACT

The utilization of various tetrazoles as efficient ligands is a promising method for the functionalization of tetrazole-based heterogeneous catalysts. Their combination with magnetic species and natural supports exposes huge opportunities for the practical applications of heterogeneous catalysts. In this study, a green and novel strategy is applied to synthesize Fe₃O₄ magnetic nanoparticles (MNPs) incorporated with chitosan (CS) and 5-amino-1*H*-tetrazole with a long tail ((3-chloropropyl)trimethoxysilane) to immobilize palladium catalyst designated as Fe₃O₄-CS@tet-Pd(II). The prepared Fe₃O₄-CS@tet-Pd(II) was used as an efficient and magnetically recyclable catalyst for the Suzuki-Miyaura cross-coupling reaction (SMCR) using a mixture of EtOH/H₂O as green media under aerobic conditions. All the expected products were obtained in high yields, indicating the high efficiency of this catalyst for the preparation of various biaryl by SMCR. Various latest techniques were used to characterize Fe₃O₄-CS@tet-Pd(II), e.g., Fourier-transform infrared spectroscopy (FT-IR), energy-dispersive X-ray spectroscopy (EDS) elemental mapping, X-ray diffraction (XRD), transmission electron microscopy (TEM), scanning TEM (STEM), high resolution TEM (HR-TEM), vibrating sample magnetometer (VSM), fast Fourier transform (FFT), thermogravimetric analysis (TGA), etc. This study presents a unique example of 5-amino-1*H*-tetrazole grafted on Fe₃O₄-CS, which can easily be separated using an external magnet and reused five times without significant decrease of catalytic activity. In addition, the introduced method has significant advantages such as the utilization of natural and inexpensive materials, easy work-up, high yields of products, and high catalytic activity.

© 2021 Elsevier B.V. All rights reserved.

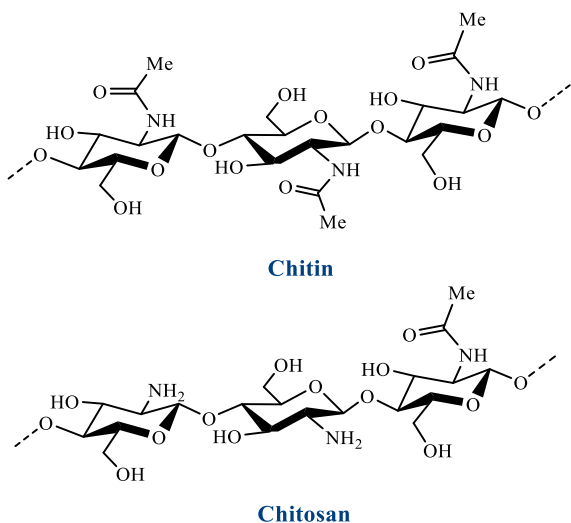
1. Introduction

Metal-catalyzed Suzuki-Miyaura coupling reaction (SMCR) is one of the most important organic reactions for the synthesis of various biaryl compounds expediting the reaction between aryl halides and arylboronic acids [1-3]. SMCR has been applied for the synthesis of polymers, pharmaceuticals, advanced materials, etc. [4,5]. Among transition metals, palladium (Pd)-based catalysts have often been utilized in the carbon-carbon bond formations, e.g., Negishi, Heck, Hiyama, Stille, Sonogashira, and, in particular, SMCR [6-10]. Consequently, there are many reports related to the

synthesis of various homogeneous or heterogeneous Pd-based catalysts and their catalytic applications to promote the aforementioned coupling reactions [11-13]. Indeed, heterogeneous Pd catalysts have better reusability and durability than homogeneous catalysts. Therefore, they are generally utilized for large-scale catalytic organic processes and industrial applications [14-16]. The incorporation of solid supports with magnetic nanoparticles (NPs) provides convenient catalyst recycling. Magnetically recyclable catalysts have various advantages including cost efficiency, environmentally benign, non-toxicity, high surface area, easy separation, etc. [17-20]. In contrast, unsupported catalyst NPs have low stability and agglomerate quickly in the reaction mixture, losing their efficiency [21-23]. To avoid their inevitable aggregation and resolve the issues of stability, leaching, separation, and recovery, many inorganic materials have been utilized as steady support

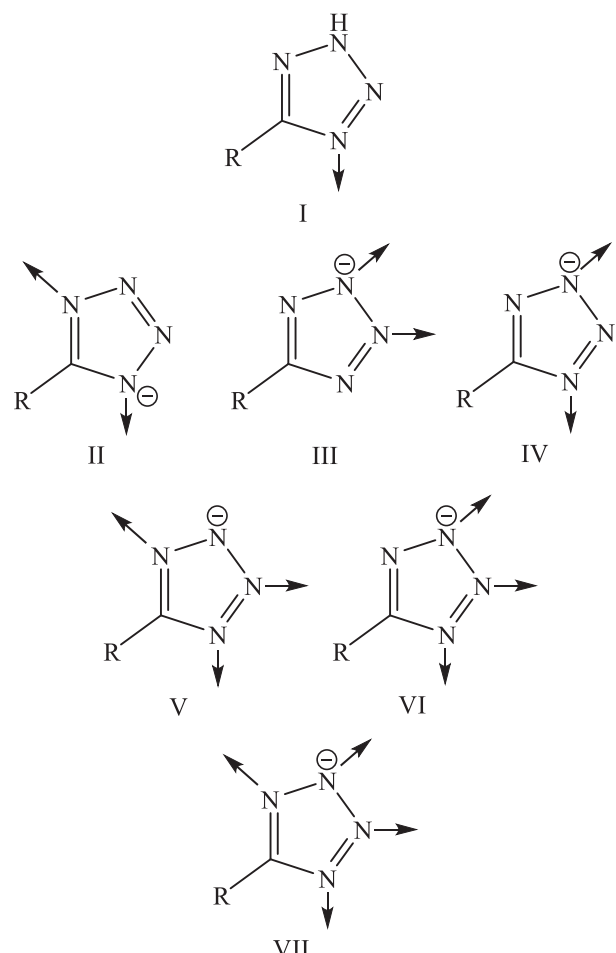
* Corresponding authors.

E-mail addresses: mahmoudnasr81@gmail.com (M. Nasrollahzadeh), yasin@njfu.edu.cn (Y. Orooji), mrsh2@snu.ac.kr (M. Shokouhimehr).

**Fig. 1.** Structures of chitin and chitosan.

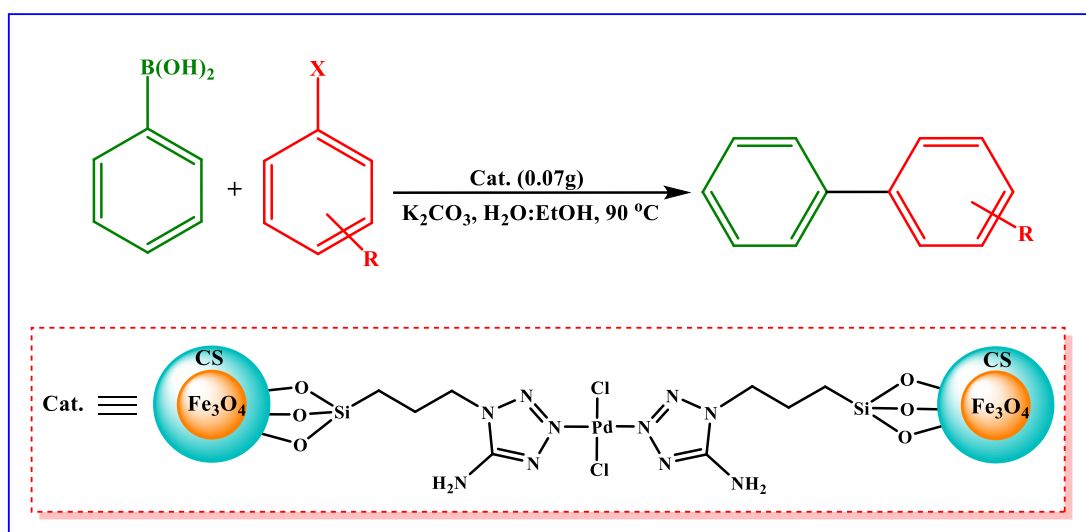
for the immobilization of catalysts, e.g., clinoptilolite [24], sodium borosilicate [25], graphene oxide [26], etc.

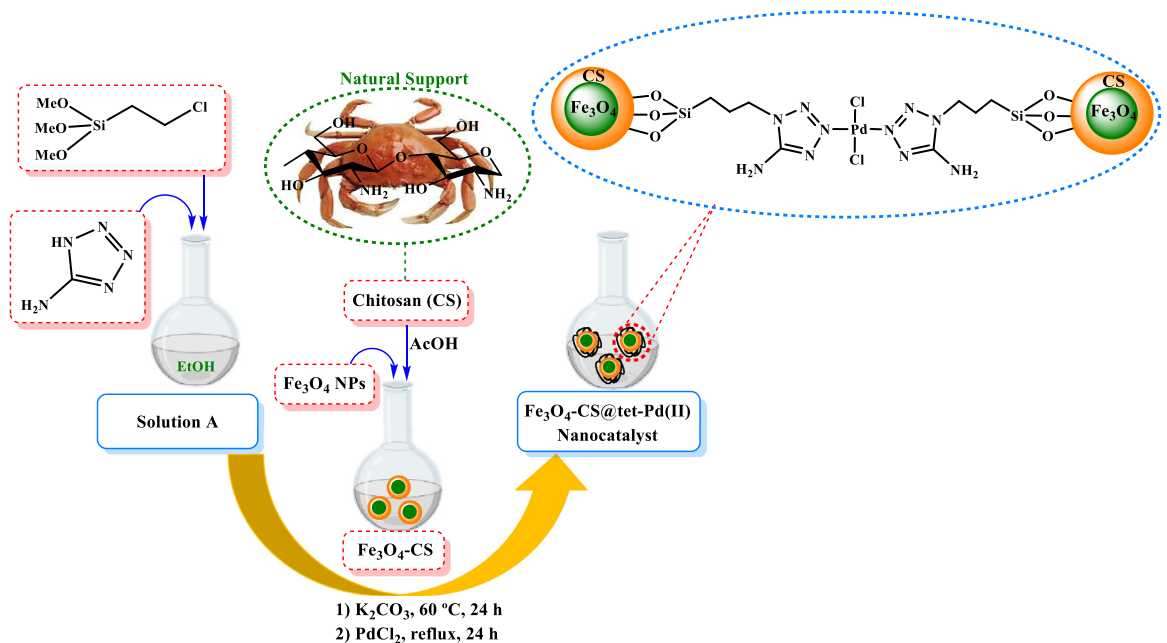
Among the available supports, biopolymers such as chitosan (CS) are used for the immobilization of metal NPs due to their excellent stability, low cost, and high surface area [27-30]. CS is a linear polysaccharide composed of randomly distributed β -(1 \rightarrow 4)-linked D-glucosamine (deacetylated unit) and N-acetyl-D-glucosamine (acetylated unit) generally obtained from alkaline deacetylation of chitin which is widely available in the exoskeleton of certain crustacea such as crab, shrimp, and crawfish [31]. Fig. 1 demonstrates the structure of chitin and chitosan [32]. In addition, CS has high biocompatibility, adsorption properties, and biodegradability [29-31,33-35]. Butnariu and co-workers investigated the Fourier-transform infrared spectroscopy (FT-IR) of chitosan and chitin extract as biomass sources, confirming the presence of OH and NH₂ groups [32]. CS also contains hydroxyl and amine groups, which can chelate with metal NPs [36-38]. Recently, the use of tetrazoles as efficient ligands in catalysis has garnered huge attention [39,40]. Tetrazoles and their anion (tetrazolate) have several coordination modes (Fig. 2), functioning as multiden-

**Fig. 2.** Coordination modes of tetrazoles and their anion.

tate ligands in coordination chemistry for the synthesis of effective catalysts via the complexation with metal ions [41-45].

In continuation of our study on the synthesis of tetrazole-based catalysts, we described a facile and effective synthesis of magnetic chitosan-supported tetrazole-Pd(II) complex ($\text{Fe}_3\text{O}_4\text{-CS@tet-Pd(II)}$).

**Scheme 1.** Synthesis procedure for the preparation of $\text{Fe}_3\text{O}_4\text{-CS@tet-Pd(II)}$ catalyst.

**Scheme 2.** Preparation procedure for Fe_3O_4 -CS@tet-Pd(II) catalyst.

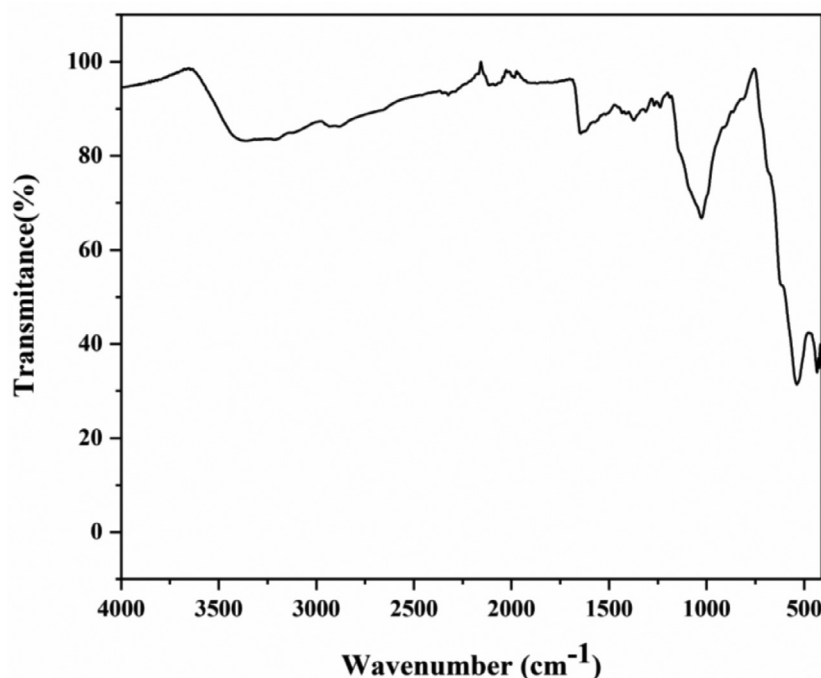
The prepared catalyst exhibited high catalytic activity for the SMCR under green reaction conditions in ethanol:water (1:1) at 90 °C (**Scheme 1**).

2. Experimental

2.1. Reagents and methods

All the chemicals and solvents applied in this work were purchased from Aldrich company and directly employed as received without further purification. FT-IR analysis determined

the functional groups using a Perkin-Elmer 781 instrument. X-ray diffraction (XRD) and vibrating sample magnetometer (VSM) measurements were performed using a Philips PW1373 ($\text{Cu K}\alpha = 1.5406 \text{ \AA}$, 2θ range = 10–90°) and Lake Shore VSM-7410, respectively. The shape, size, composition, and elemental distribution of Fe_3O_4 -CS@tet-Pd(II) were analyzed by transmission electron microscopy (TEM), scanning TEM (STEM), high resolution TEM (HR-TEM) using a JEM-F200 JEOL microscope equipped with energy-dispersive X-ray spectroscopy (EDS). The thermal analysis of Fe_3O_4 -CS@tet-Pd(II) was carried out by thermogravimetric analysis (TGA, Discovery USA) under nitrogen atmosphere. A Bruker

**Fig. 3.** FT-IR of Fe_3O_4 -CS@tet-Pd(II).

Advance DRX500 MHz spectrometer was used to record ^1H NMR spectra. Melting points were measured on a BUCHI 510 melting point apparatus.

2.2. Synthesis of Fe_3O_4 -chitosan

Fe_3O_4 -chitosan (Fe_3O_4 -CS) was prepared following the procedure of our recently published article [30]. To prepare Fe_3O_4 -CS (0.25 g) was dissolved in acetic acid solution (1%, 50 mL) and mixed with Fe_3O_4 NPs (2 g). The mixture was stirred for ~1 h. Then, NaOH solution (50 mL, 1.0 M) was added slowly to the mixture while stirring. The solid product (Fe_3O_4 -CS) was isolated by an external magnet.

2.3. Synthesis of Fe_3O_4 -CS@5-amino-1H-tetrazole (Fe_3O_4 -CS@tet)

The synthetic procedure for the preparation of Fe_3O_4 -CS@tet is shown in Scheme 2. 5-amino-1H-tetrazole (5 mmol) was dissolved in ethanol (50 mL), and (3-chloropropyl)trimethoxysilane (5 mmol) was added to the mixture under stirring. The mixture was stirred for 24 h under reflux conditions (solution A). Subsequently, Fe_3O_4 -CS (1.5 g) was dispersed in ethanol (70 mL) using sonication for 20 min and mixed with solution A and K_2CO_3 (5 mmol). The obtained mixture was stirred for 24 h at 60 °C. Then, Fe_3O_4 -CS@tet was collected with an external magnet and thoroughly washed with ethanol several times, and finally dried in a vacuum oven at 60 °C for 12 h.

2.4. Synthesis of Fe_3O_4 -CS@tet-Pd(II)

To prepare Fe_3O_4 -CS@tet-Pd(II), a mixture of the as-prepared Fe_3O_4 -CS@tet (1 g) and PdCl_2 (0.5 g) in ethanol (50 mL) was stirred under reflux conditions for 24 h. The obtained solid product was collected with an external magnet, washed with ethanol several times, and dried in a vacuum oven at 60 °C. The prepared nanostructured catalyst was utilized in SMCR (Scheme 2).

2.5. General procedure for the Suzuki-Miyaura coupling reaction

A mixture of aryl halide (1 mmol), $\text{C}_6\text{H}_5\text{B}(\text{OH})_2$ (1.1 mmol), K_2CO_3 (2.0 mmol), and Fe_3O_4 -CS@tet-Pd(II) catalyst (0.07 g) in 8 mL EtOH:H₂O (1:1) was stirred at 90 °C. The reaction progress was monitored by thin-layer chromatography (TLC). After completion of the reaction, the catalyst was removed by an external magnet, washed with ethanol and dried at 70 °C, and reused for the subsequent reaction cycle. The synthesized compounds were purified using column chromatography on silica gel and characterized by nuclear magnetic resonance (NMR) and melting point analysis.

2.6. Characterization data of selected product

Biphenyl

^1H NMR (500 MHz, CDCl_3) $\delta_{\text{H}} = 7.67$ (d, $J = 9.1$ Hz, 2H), 7.52 (t, $J = 9.1$ Hz, 2H), 7.43 (d, $J = 8.8$ Hz, 1H).

3. Results and discussion

3.1. Characterization of Fe_3O_4 -CS@tet-Pd(II) catalyst

Fe_3O_4 -CS@tet-Pd(II) catalyst was characterized precisely using FT-IR, EDS, elemental mapping, XRD, STEM, HR-TEM, VSM, and TGA techniques. Fig. 3 shows the FT-IR spectrum of Fe_3O_4 -CS@tet-Pd(II)

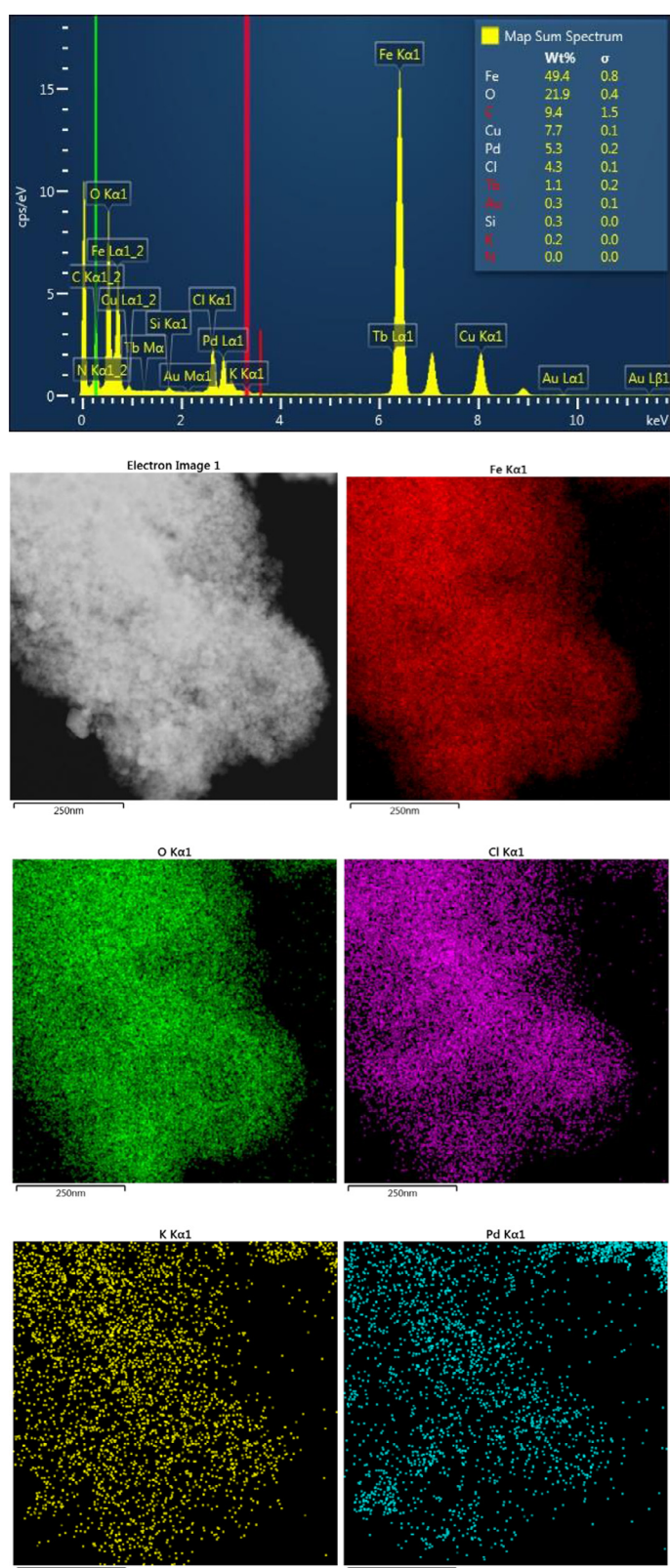


Fig. 4. EDS spectrum and elemental mapping of Fe_3O_4 -CS@tet-Pd(II) catalyst.

catalyst. A sharp peak appeared at 1644 cm^{-1} presents the C = N stretching vibration. As shown in Fig. 1, the broad peak at 3200 – 3500 cm^{-1} is related to the stretching vibrations of -OH and/or -NH in chitosan. The construction peak of Fe_3O_4 is observed at 536 cm^{-1} , where the Fe-O stretching vibration is clear for Fe_3O_4 MNPs [46]. The absorption peaks at 1026 , 790 , and 434 cm^{-1} indicate

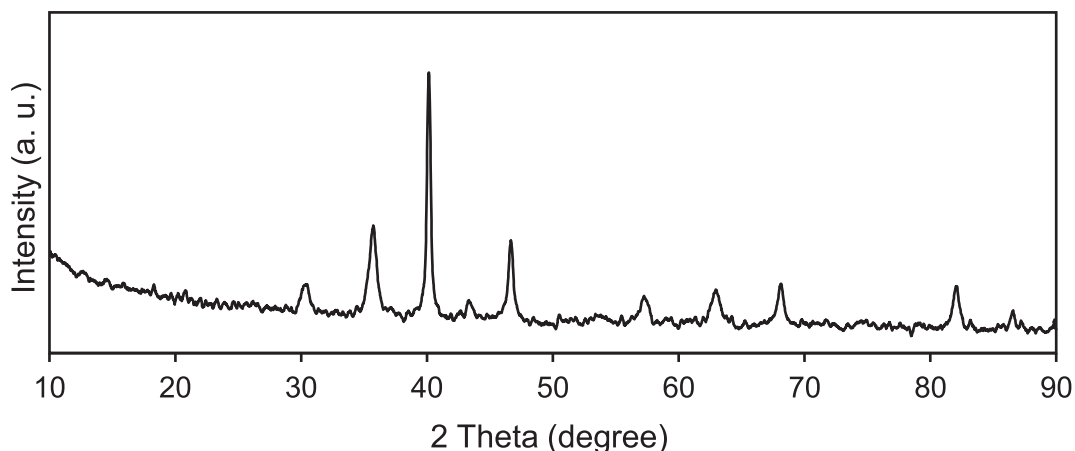


Fig. 5. XRD pattern of $\text{Fe}_3\text{O}_4\text{-CS@tet-Pd(II)}$ catalyst.

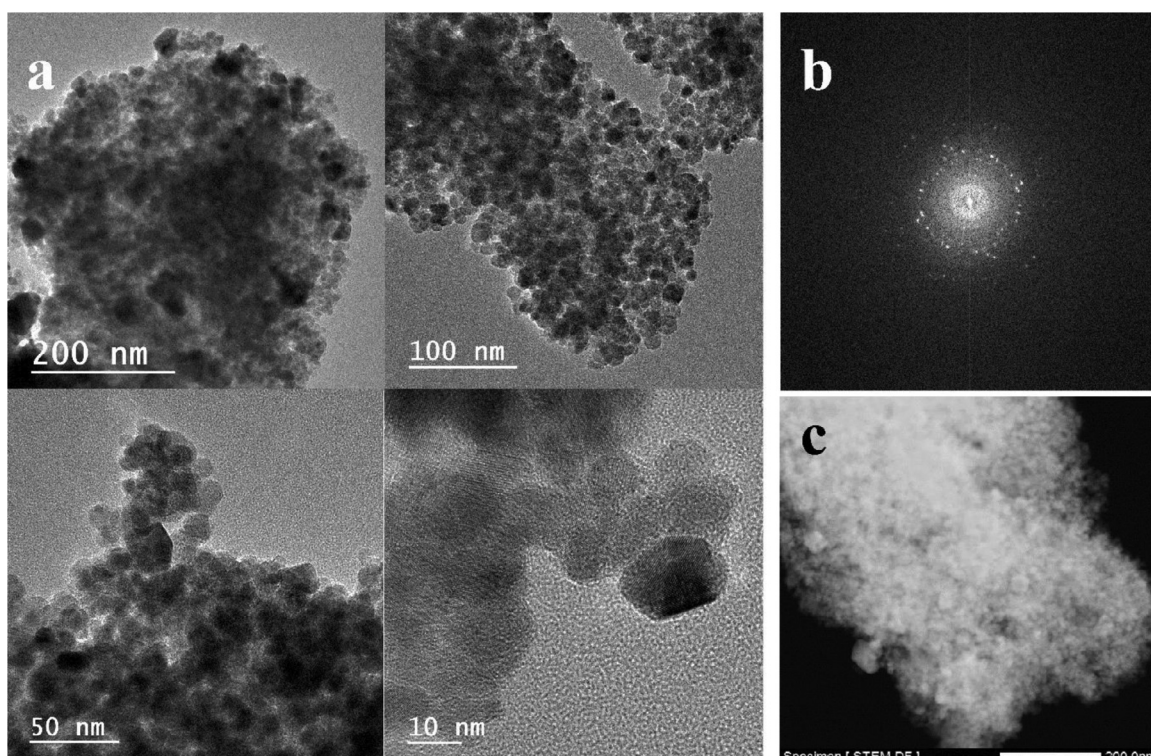


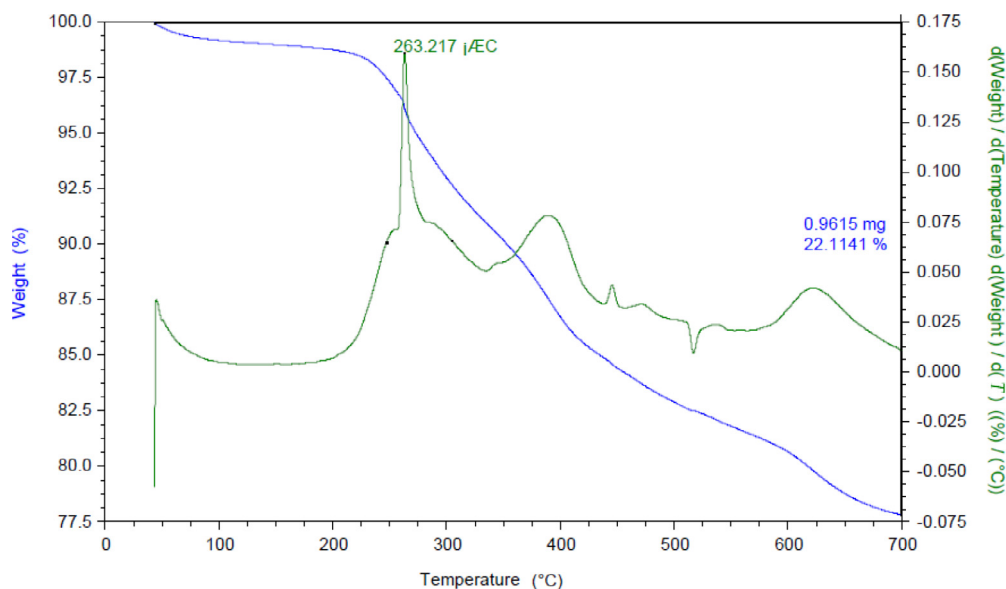
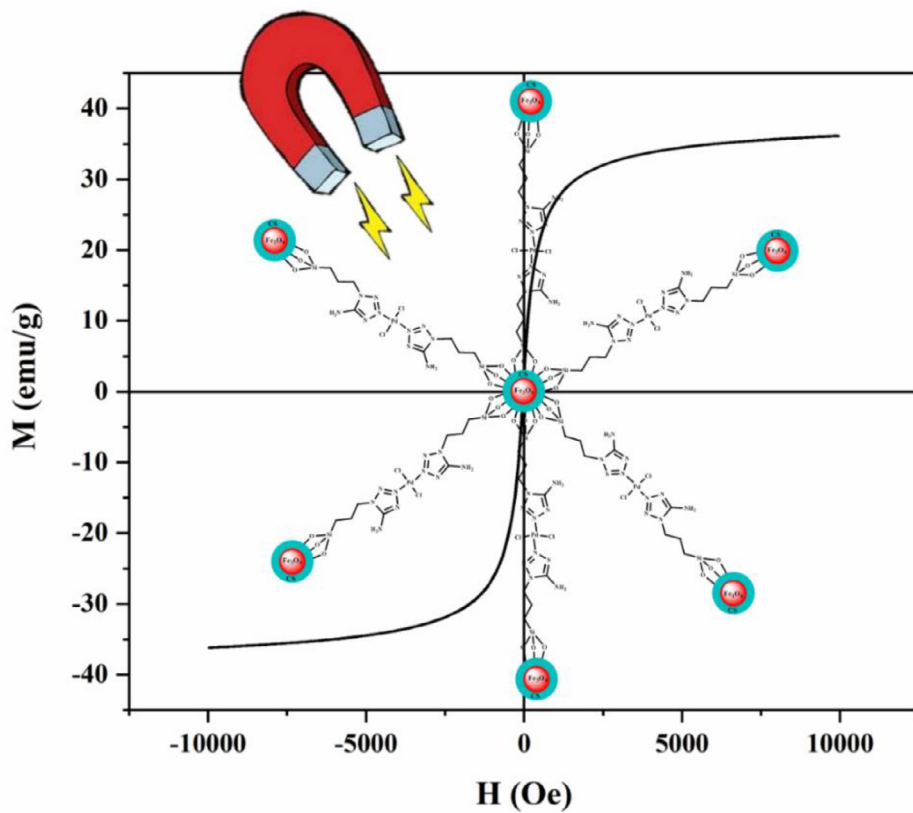
Fig. 6. (a) TEM and HR-TEM, (b) FFT, and (c) STEM images of $\text{Fe}_3\text{O}_4\text{-CS@tet-Pd(II)}$ catalyst.

the Si-O-Si stretching, Si-O bending, and Si-O-Si bending, respectively. The characteristic absorption bands $\sim 2800\text{--}3000\text{ cm}^{-1}$ and $1400\text{--}1500\text{ cm}^{-1}$ are attributed to C-H stretching and bending vibrations of CH_2 [40]. In addition, the band at 1450 cm^{-1} is ascribed to the N = N stretching vibration in the structure of 5-amino-1*H*-tetrazole.

The chemical composition of $\text{Fe}_3\text{O}_4\text{-CS@tet-Pd(II)}$ catalyst was characterized by EDS elemental mapping analysis (Fig. 4). Distinct peaks of Fe, C, N, Si, O, Pd, and Cl are clearly observed in the EDS spectrum, indicating the formation and integrity of $\text{Fe}_3\text{O}_4\text{-CS@tet-Pd(II)}$ catalyst. Furthermore, the presence of Pd and other elements existing in $\text{Fe}_3\text{O}_4\text{-CS@tet-Pd(II)}$ confirms the grafting of the palladium(II)-N-heterocyclic complex onto the surface of $\text{Fe}_3\text{O}_4\text{-CS}$.

The structure of $\text{Fe}_3\text{O}_4\text{-CS@tet-Pd(II)}$ catalyst was determined by XRD study, confirming the presence of Fe_3O_4 and Pd NPs. As seen in Fig. 5, the sharp diffraction peaks indicate the high crystallinity of $\text{Fe}_3\text{O}_4\text{-CS@tet-Pd(II)}$ catalyst. The characteristic peaks at $2\theta = 30.2^\circ, 35.7^\circ, 43.4^\circ, 53.8^\circ, 57.4^\circ$, and 63.1° can be assigned to (220), (311), (400), (422), (511) and (440) reflection planes, respectively, which are in good agreement to the cubic magnetite phase (JCPDS#01-075-0449) of The peaks observed at 40.1° (111), 46.7° (200), and 68.2° (220) are corresponding to the face-centered cubic structure of Pd NPs in $\text{Fe}_3\text{O}_4\text{-CS@tet-Pd(II)}$ catalyst, assuring their immobilization on $\text{Fe}_3\text{O}_4\text{-CS}$.

The morphology of $\text{Fe}_3\text{O}_4\text{-CS@tet-Pd(II)}$ catalyst was studied by TEM, HR-TEM, STEM, and fast Fourier transform (FFT) analyses (Fig. 6a-c). Fig. 6a demonstrates the TEM and HR-TEM images of

**Fig. 7.** TGA curve of $\text{Fe}_3\text{O}_4\text{-CS@tet-Pd(II)}$ catalyst.**Fig. 8.** VSM curve of $\text{Fe}_3\text{O}_4\text{-CS@tet-Pd(II)}$.

the as-prepared $\text{Fe}_3\text{O}_4\text{-CS@tet-Pd(II)}$ with different magnifications. It can be clearly seen from Fig. 6a that the obtained Pd NPs possess spherical shape and are moderately uniform, dispersing with an average diameter of ~10 nm. To further verify the crystallinity and well-dispersion of Pd NPs on the surface of $\text{Fe}_3\text{O}_4\text{-CS@tet}$, STEM and FFT images were investigated (Fig. 6b). As shown in Fig. 7c,

the STEM image unambiguously demonstrates a homogeneously assembled nanostructured catalyst.

Thermal stability of $\text{Fe}_3\text{O}_4\text{-CS@tet-Pd(II)}$ catalyst was analyzed by TGA analysis. Fig. 7 illustrates the comparative weight loss of $\text{Fe}_3\text{O}_4\text{-CS}$ magnetic NPs and Pd(II)-5-amino-1H-tetrazole complex immobilized on the modified magnetic NPs. The TGA curve depicts

Table 1
Optimization of the reaction conditions for SMCR.^a

Entry	Solvent	Catalyst (g)	Base	Time (h)	Yield (%) ^b
1	H ₂ O	Fe ₃ O ₄ -CS@tet-Pd(II) (0.05)	K ₂ CO ₃	4.5	48
2	EtOH	Fe ₃ O ₄ -CS@tet-Pd(II) (0.05)	K ₂ CO ₃	3.5	67
3	Glycerol	Fe ₃ O ₄ -CS@tet-Pd(II) (0.05)	K ₂ CO ₃	3.5	79
4	EtOH/H ₂ O	Fe ₃ O ₄ -CS@tet-Pd(II) (0.05)	K ₂ CO ₃	1.5	81
5	EtOH/H ₂ O	Fe ₃ O ₄ -CS@tet-Pd(II) (0.05)	Na ₂ CO ₃	3	76
6	EtOH/H ₂ O	Fe ₃ O ₄ -CS@tet-Pd(II) (0.05)	Et ₃ N	2:45	77
7	EtOH/H ₂ O	Fe ₃ O ₄ -CS@tet-Pd(II) (0.05)	NaOH	4:35	77
8	EtOH/H₂O	Fe₃O₄-CS@tet-Pd(II) (0.07)	K₂CO₃ 1:10		92
9	EtOH/H ₂ O	Fe ₃ O ₄ -CS@tet-Pd(II) (0.05)	K ₂ CO ₃	4	0
10	EtOH/H ₂ O	Fe ₃ O ₄ -CS@tet-Pd(II) (0.04)	K ₂ CO ₃	4	74
11	EtOH/H ₂ O	Fe ₃ O ₄ -CS@tet-Pd(II) (0.05)	—	4	Trace
12	EtOH/H ₂ O	Fe ₃ O ₄ -CS@tet-Pd(II) (0.08)	K ₂ CO ₃	1:10	92

^a Reaction conditions: PhB(OH)₂ (1.1 mmol), iodobenzene (1.0 mmol), base (2.0 mmol), and solvent (8.0 mL) at 90 °C.

^b Isolated yields.

Table 2
SMCR of phenylboronic acid with different aryl halides catalyzed by Fe₃O₄-CS@tet-Pd(II) catalyst.^a

Entry	R	X	Time (min)	Yield (%) ^b
1	H	I	70	92
2	2-OMe	I	70	88
3	4-OMe	I	70	89
4	4-Me	I	70	88
5	3-NO ₂	I	70	85
6	4-COMe	I	70	90
7	H	Br	130	91
8	4-OMe	Br	130	87
9	4-Me	Br	130	87
10	3-NO ₂	Br	130	78
11	4-COMe	Br	130	86
12	4-CN	Br	130	82
13	H	Cl	5 h	76
14	4-OMe	Cl	5 h	65

^a Reaction conditions: PhB(OH)₂ (1.1 mmol), aryl halide (1.0 mmol), Fe₃O₄-CS@tet-Pd(II) (0.07 g), and K₂CO₃ (2.0 mmol) in EtOH:H₂O (1:1, 8.0 mL) at 90 °C.

^b Isolated yields.

several weight loss steps at a heating rate of 2 °C min⁻¹ in flowing air for Fe₃O₄-CS@tet-Pd(II). The maximum thermal degradation of Fe₃O₄-CS@tet-Pd(II) catalyst was observed at 263 °C. The initial weight loss, from the room temperature to 210 °C, is related to the removal of physically adsorbed molecular water and organic solvents on the surface of the catalyst. Most weight loss occurs above 230 °C (between 230 and 600 °C), which is related to the degradation of organic functional groups such as tetrazole and modified magnetic NPs. In addition, a weight loss is observed above 600 °C, which is assigned to the complete decomposition of the catalyst.

The magnetic properties of Fe₃O₄-CS@tet-Pd(II) catalyst were examined using VSM technique at room temperature in a field sweeping from -10⁴ to +10⁴ Oe (Fig. 8). Fe₃O₄-CS@tet-Pd(II) catalyst presents a sensitive magnetic response so that it can easily be separated from the reaction mixture by using an external magnet. The magnetization of Fe₃O₄ NPs is higher than Fe₃O₄-CS@tet-Pd(II) catalyst due to the modification of Fe₃O₄ NPs with chitosan support and tetrazole ligand. However, the magnetic property of Fe₃O₄-CS@tet-Pd(II) catalyst is sufficiently high to provide efficient separation and recycle.

3.2. Catalytic activity of Fe₃O₄-CS@tet-Pd(II) for the synthesis of biaryl derivatives

The efficiency of Fe₃O₄-CS@tet-Pd(II) catalyst was tested for the ligand-free SMCR. This catalyst eliminates the need for expensive and moisture-sensitive ligands for SMCR achievement. To optimize the reaction conditions, the reaction between iodobenzene (1 mmol) and phenylboronic acid (1.1 mmol) was chosen as a model reaction using Fe₃O₄-CS@tet-Pd(II) catalyst at 90 °C (Table 1). Several experiments were performed under different reaction conditions (nature of the base, effect of solvent, amount of catalyst, etc.). The efficiency of the catalyst loading on the production of biphenyl was studied by various amounts of Fe₃O₄-CS@tet-Pd(II) in the presence of various bases (e.g., K₂CO₃, Na₂CO₃, NEt₃, and NaOH) and solvents (e.g., Glycerol, EtOH, H₂O, and EtOH/H₂O). According to the obtained results, no product was obtained in the absence of Fe₃O₄-CS@tet-Pd(II) or the presence of Fe₃O₄-CS@tet (entry 9). It was found that the best yield was produced using K₂CO₃ (2 mmol) and EtOH/H₂O (1:1, 8.0 mL) as the base and solvent, respectively, as presented in Table 1. The amount of Fe₃O₄-CS@tet-Pd(II) varied in the range of 0.04–0.07 g in the presence of K₂CO₃ and EtOH/H₂O at 90 °C. The maximum yield of the

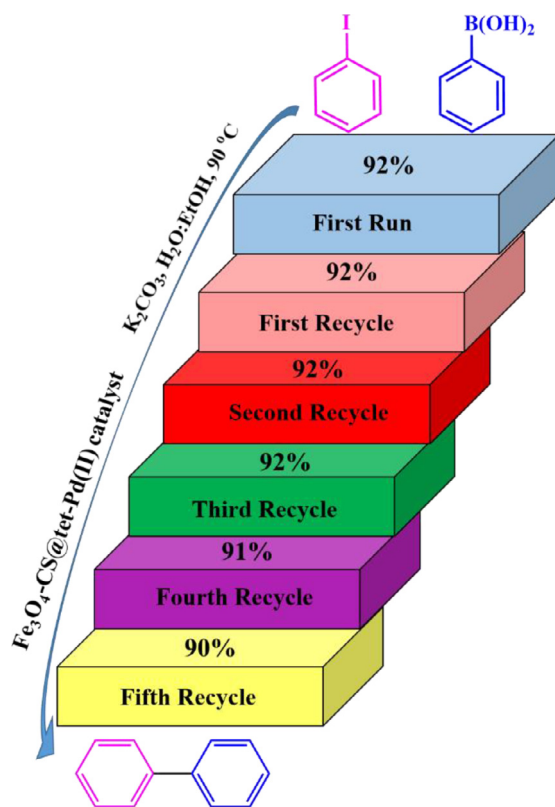


Fig. 9. Reusability of $\text{Fe}_3\text{O}_4\text{-CS@tet-Pd(II)}$ catalyst for SMCR of $\text{PhB}(\text{OH})_2$ and iodobenzene.

desired product was obtained in the presence of $\text{Fe}_3\text{O}_4\text{-CS@tet-Pd(II)}$ catalyst (0.07 g) (Table 1, entry 8). No further improvement in the yield of the product was discerned by increasing the amount of $\text{Fe}_3\text{O}_4\text{-CS@tet-Pd(II)}$ to 0.08 g (entry 13). Based on these observations, it was concluded that the optimum reaction condition was K_2CO_3 (2 mmol) and catalyst (0.07 g) in $\text{EtOH}/\text{H}_2\text{O}$ at 90 °C temperature (Table 1, entry 8).

Under the optimized conditions, the catalytic activity, generality, and scope of the as-prepared $\text{Fe}_3\text{O}_4\text{-CS@tet-Pd(II)}$ catalyst was explored for the synthesis of biaryl derivatives using a variety of aryl halides and phenylboronic acid (Table 2). The reaction of $\text{PhB}(\text{OH})_2$ with various aryl halides containing electron-withdrawing and electron-donating groups provided different derivatives of biaryls yielding 82–92% within 70 min to 5 h using 0.07 g of $\text{Fe}_3\text{O}_4\text{-CS@tet-Pd(II)}$ catalyst in $\text{EtOH}:\text{H}_2\text{O}$ (1:1, 8.0 mL) at 90 °C (Table 2). In addition, iodobenzenes were obtained in good yields (Table 2, entry 1–6). To further investigate the efficacy of $\text{Fe}_3\text{O}_4\text{-CS@tet-Pd(II)}$ catalyst, the reaction of chlorobenzene and 4-methylchlorobenzene with phenylboronic acid was examined. Under the optimized reaction conditions, the corresponding products were obtained in good yields (Table 2, entries 13 and 14).

3.3. Catalyst reusability

The recyclability of $\text{Fe}_3\text{O}_4\text{-CS@tet-Pd(II)}$ catalyst was studied in a model reaction of iodobenzene and phenylboronic acid in the presence of K_2CO_3 as an effective base in $\text{EtOH}:\text{H}_2\text{O}$ at 90 °C. After completion of the reaction as monitored by TLC, the reaction mixture was cooled down to room temperature and the catalyst was separated by an external magnet, washed with ethanol, and dried in an oven at 70 °C. Then, the catalyst was reused for the next cycles. It was found that the catalyst exhibited superb catalytic ac-

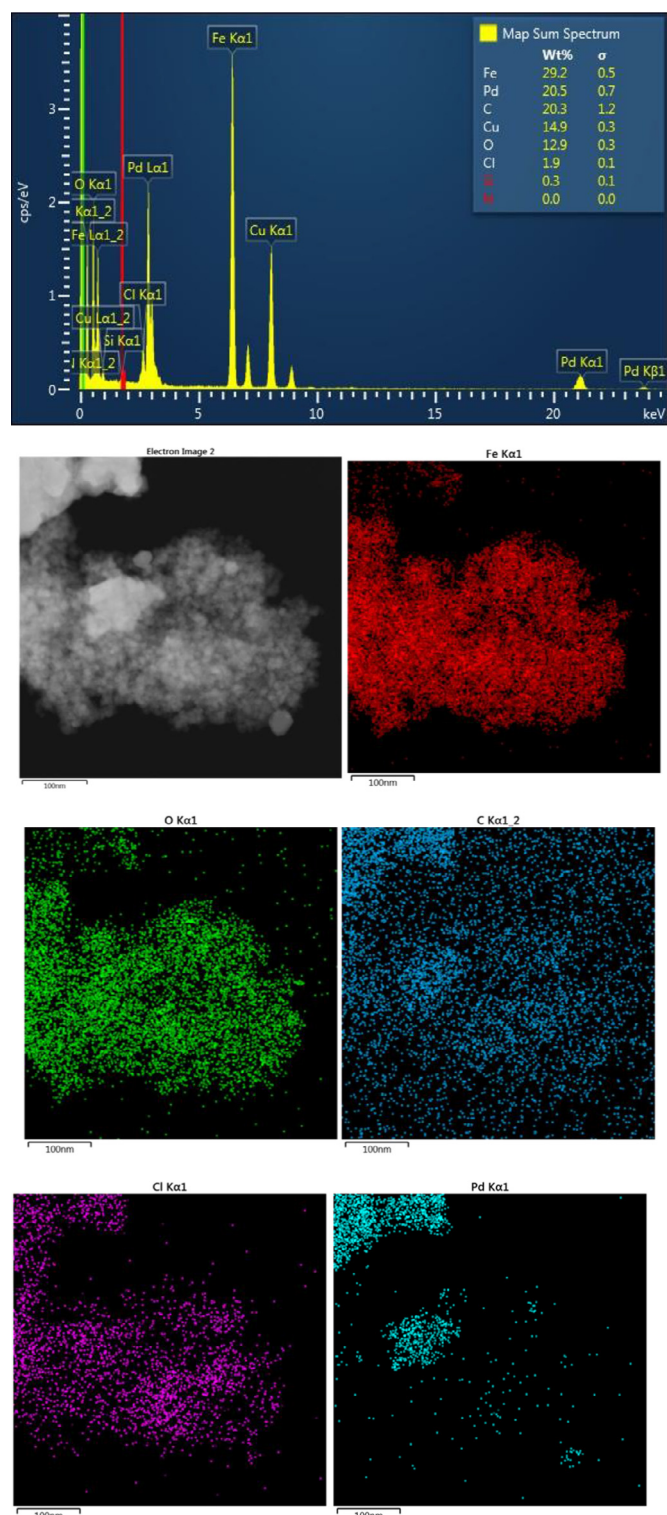


Fig. 10. EDS image and elemental mapping of recycled $\text{Fe}_3\text{O}_4\text{-CS@tet-Pd(II)}$ catalyst.

tivity even after five runs without any significant loss of activity (Fig. 9), indicating the high stability and efficiency of the catalyst under the applied reaction conditions. The EDS elemental mapping, TEM, and HRTEM analyses of the recovered $\text{Fe}_3\text{O}_4\text{-CS@tet-Pd(II)}$ catalyst after five runs are shown in Figs. 10 and 11. These results indicate that the size and shape of the catalyst are retained without obvious detectable changes in the morphology and chemical structure.

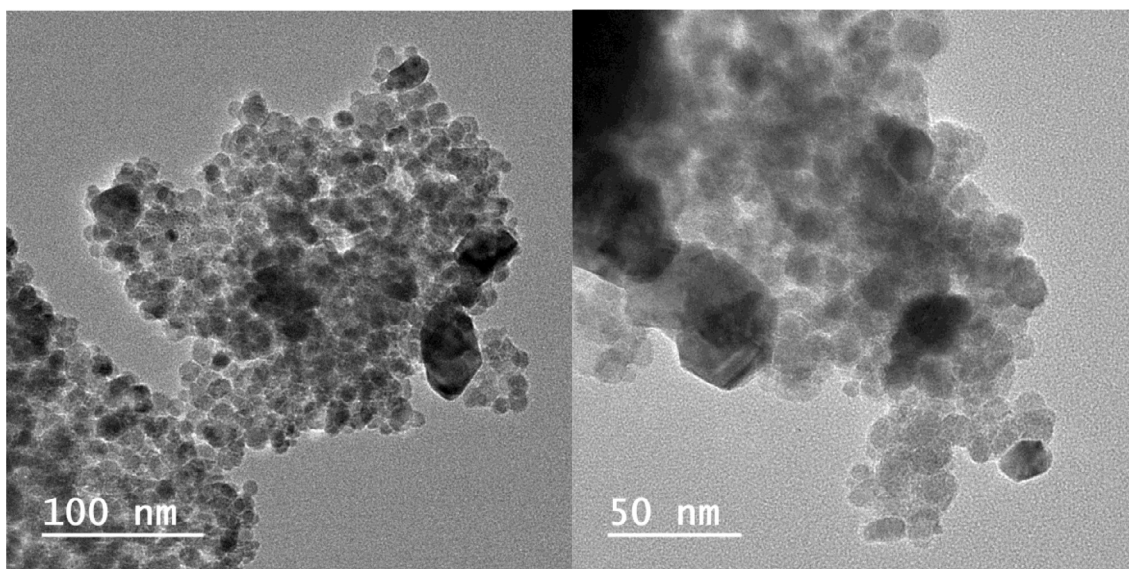


Fig. 11. TEM and HR-TEM images of the recycled $\text{Fe}_3\text{O}_4\text{-CS@tet-Pd(II)}$ catalyst.

4. Conclusions

Tetrazoles have been used as efficient ligands for the preparation of various catalysts due to their wide applicability, high stability, complexation with different metals, and low toxicity. This research describes a novel, environmentally benign, efficient, and low-cost method for SMCR using a highly active and reusable catalyst consists of chitosan as a natural support for the functionalization of the tetrazole-Pd(II) complex. This catalyst was precisely characterized using FT-IR, EDS, XRD, STEM, HR-TEM, VSM, and TGA techniques. The SMCR was performed for the reaction of aryl halides with phenylboronic acid in the presence of $\text{Fe}_3\text{O}_4\text{-CS@tet-Pd(II)}$ catalyst, K_2CO_3 , and $\text{EtOH:H}_2\text{O}$ as a green solvent at 90°C . Various substituted aryl halides were employed to obtain the desirable biaryls. This nanostructured catalyst presented several advantages, e.g., provided high yields of products, and prepared by natural, inexpensive, and nontoxic materials, etc. In addition, its high efficiency in green solvents (ethanol and water mixture) and simple recycling protocol by applying an external magnetic field expose this catalyst as a promising candidate for the goal of green chemistry. The recovered catalyst also presented high stability and activity as confirmed by various characterizations (e.g., EDS elemental mapping, TEM, and HRTEM). In addition, this novel method may find a promising future in the development of tetrazole-based catalysts due to the existence of broad tetrazole ligands library.

Declaration of Competing Interest

The authors declare no competing interest.

Acknowledgments

We gratefully acknowledge the University of Qom for the support of this work. We appreciate Nanjing Forestry University (Grant Nos. 163020211 and 163020816), and Symbolic Achievement Cultivation Project (grant number 163020139) for the financial support. This research was supported by the National Research Foundation of Korea (NRF) funded by the Ministry of Science and ICT (2020M2D8A206983011). Furthermore, the financial supports of the Basic Science Research Program (2017R1A2B3009135) through the National Research Foundation of Korea is appreciated.

References

- [1] S.R. Chemler, D. Trauner, S.J. Danishefsky, The B-alkyl Suzuki-Miyaura cross-coupling reaction: development, mechanistic study, and applications in natural product synthesis, *Angew. Chem. Int. Ed.* 40 (2001) 4544–4568.
- [2] R. Martin, S.L. Buchwald, Palladium-catalyzed Suzuki-Miyaura cross-coupling reactions employing dialkylbiaryl phosphine ligands, *Acc. Chem. Res.* 41 (2008) 1461–1473.
- [3] S. Shi, S.P. Nolan, M. Szostak, Well-defined palladium(II)-NHC precatalysts for cross-coupling reactions of amides and esters by selective N-C/O-C cleavage, *Acc. Chem. Res.* 51 (2018) 2589–2599.
- [4] M. Kertesz, C.H. Choi, S. Yang, Conjugated polymers and aromaticity, *Chem. Rev.* 105 (2005) 3448–3481.
- [5] M. Gómez-Martínez, A. Baeza, D.A. Alonso, Graphene oxide-supported oxime palladacycles as efficient catalysts for the Suzuki-Miyaura cross-coupling reaction of aryl bromides at room temperature under aqueous conditions, *Catalysts* 7 (2017) 94.
- [6] X. Duan, M. Xiao, S. Liang, Z. Zhang, Y. Zeng, J. Xi, S. Wang, Ultrafine palladium nanoparticles supported on nitrogen-doped carbon microtubes as a high-performance organocatalyst, *Carbon* 119 (2017) 326–331.
- [7] A. Biffis, P. Centomo, A. Del Zotto, M. Zecca, Pd metal catalysts for cross-couplings and related reactions in the 21st century: a critical review, *Chem. Rev.* 118 (2018) 2249–2295.
- [8] T.J. Colacot, New Trends in cross-coupling: Theory and Applications, Royal Society of Chemistry, Cambridge, U.K., 2014.
- [9] T. Baran, M. Nasrollahzadeh, Z. Issaabadi, M.M. Tohidi, S.M. Sajadi, Facile synthesis of palladium nanoparticles immobilized on magnetic biodegradable microcapsules used as effective and recyclable catalyst in Suzuki-Miyaura reaction and p-nitrophenol reduction, *Carbohydr. Polym.* 222 (2019) 115029.
- [10] X. Duan, J. Liu, J. Hao, L. Wu, B. He, Y. Qiu, J. Zhang, Z. He, J. Xi, S. Wang, Magnetically recyclable nanocatalyst with synergistic catalytic effect and its application for 4-nitrophenol reduction and Suzuki coupling reactions, *Carbon* 130 (2018) 806–813.
- [11] R. Chinchilla, C. Najera, Recent advances in Sonogashira reactions, *Chem. Soc. Rev.* 40 (2011) 5084–5121.
- [12] J.-H. Kim, J.-W. Kim, M. Shokouhimehr, Y.-S. Lee, Polymersupported N-heterocyclic carbene-palladium complex for heterogeneous Suzuki cross-coupling reaction, *J. Org. Chem.* 70 (2005) 6714–6720.
- [13] M. Shokouhimehr, J.-H. Kim, Y.-S. Lee, Heterogeneous Heck reaction catalyzed by recyclable polymer-supported N-heterocyclic carbene-palladium complex, *Synlett* (2006) 0618–0620.
- [14] T. Baran, T. Inanan, A. Menteş, Synthesis, characterization, and catalytic activity in Suzuki coupling and catalase-like reactions of new chitosan supported Pd catalyst, *Carbohydr. Polym.* 145 (2016) 20–29.
- [15] T. Baran, E. Akıksöz, A. Menteş, Carboxymethyl chitosan Schiff base supported heterogeneous palladium(II) catalysts for Suzuki cross-coupling reaction, *J. Mol. Catal. A Chem.* 407 (2015) 47–52.
- [16] C. Vargas, A.M. Balu, J.M. Campelo, C. Gonzalez-Arellano, R. Luque, A.A. Romero, Towards greener and more efficient C-C and C-heteroatom couplings: present and future, *Curr. Org. Synth.* 7 (6) (2010) 568–586.
- [17] R.A. Harris, Chemotherapy drug temozolomide adsorbed onto iron-oxide (Fe_3O_4) nanoparticles as nanocarrier: a simulation study, *J. Mol. Liq.* 288 (2019) 111084.

- [18] W. Xie, Y. Xiong, H. Wang, Fe_3O_4 -poly(AGE-DVB-GMA) composites immobilized with guanidine as a magnetically recyclable catalyst for enhanced biodiesel production, *Renew. Energy* 174 (2021) 758–768.
- [19] S. Khashan, S. Dagher, N. Tit, A. Alazzam, I. Obaidat, Novel method for synthesis of $\text{Fe}_3\text{O}_4@\text{TiO}_2$ core/shell nanoparticles, *Surf. Coat. Technol.* 322 (2017) 92–98.
- [20] Y. Orooji, S. Mortazavi-Derazkola, S.M. Ghoreishi, M. Amiri, M. Salavati-Niasari, Mesoporous $\text{Fe}_3\text{O}_4@\text{SiO}_2$ -hydroxyapatite nanocomposite: green sonochemical synthesis using strawberry fruit extract as a capping agent, characterization and their application in sulfasalazine delivery and cytotoxicity, *J. Hazard. Mater.* 400 (2020) 123140.
- [21] A.S.M. Wittmar, Q. Fu, M. Ulbricht, Photocatalytic and magnetic porous cellulose-based nanocomposite films prepared by a green method, *ACS Sustainable Chem. Eng.* 5 (2017) 9858–9868.
- [22] E. Rezaee Nezhad, E. Pourmalekshahi, Si-Imidazole-HSO₄ functionalized magnetic Fe_3O_4 nanoparticles as an efficient and reusable catalyst for the regioselective ring opening of epoxides in water, *Nanochem. Res.* 1 (2016) 108–117.
- [23] W.F. Ma, Y. Zhang, L.L. Li, L.J. You, P. Zhang, Y.T. Zhang, J.M. Li, M. Yu, J. Guo, H.J. Lu, Tailor-made magnetic $\text{Fe}_3\text{O}_4@m\text{TiO}_2$ microspheres with a tunable mesoporous anatase shell for highly selective and effective enrichment of phosphopeptides, *ACS Nano* 6 (2012) 3179.
- [24] B. Khodadadi, M. Bordbar, A. Yeganeh-Faal, M. Nasrollahzadeh, R.J. Davis, Green synthesis of Ag nanoparticles/clinoptilolite using *Vaccinium macrocarpon* fruit extract and its excellent catalytic activity for reduction of organic dyes, *J. Alloys Compd.* 719 (2017) 82–88.
- [25] M. Nasrollahzadeh, M. Sajjadi, M. Maham, S.M. Sajadi, A.A. Barzinjy, Biosynthesis of the palladium/sodium borosilicate nanocomposite using *Euphorbia milii* extract and evaluation of its catalytic activity in the reduction of chromium(VI), nitro compounds and organic dyes, *Mater. Res. Bull.* 102 (2018) 24–35.
- [26] A. Omidvar, M.R. Rashidian Vaziri, B. Jaleh, N.P. Shabestari, M. Noroozi, Metal-enhanced fluorescence of graphene oxide by palladium nanoparticles in the blue-green part of the spectrum, *Chin. Phys. B* 25 (11) (2016) 118102.
- [27] K. Karakas, A. Celebioglu, M. Celebi, T. Uyar, M. Zahmakiran, Nickel nanoparticles decorated on electrospun polycaprolactone/chitosan nanofibers as flexible, highly active and reusable nanocatalyst in the reduction of nitrophenols under mild conditions, *Appl. Catal. B* 203 (2017) 549–562.
- [28] F. Ali, S.B. Khan, T. Kamal, K.A. Alamry, E.M. Bakhsh, A.M. Asiri, T.R.A. Sobahi, Synthesis and characterization of metal nanoparticles template chitosan-SiO₂ catalyst for the reduction of nitrophenols and dyes, *Carbohydr. Polym.* 192 (2018) 217–230.
- [29] H. Negi, P. Verma, R.K. Singh, A comprehensive review on the applications of functionalized chitosan in petroleum industry, *Carbohydr. Polym.* 266 (2021) 118125.
- [30] N. Motahharifar, M. Nasrollahzadeh, A. Taheri-Kafrani, R.S. Varma, M. Shokouhimehr, Magnetic chitosan-copper nanocomposite: a plant assembled catalyst for the synthesis of amino-and *N*-sulfonyl tetrazoles in eco-friendly media, *Carbohydr. Polym.* 232 (2020) 115819.
- [31] M. Kostag, O.A. El Seoud, Sustainable biomaterials based on cellulose, chitin and chitosan composites - A review, *Carbohydr. Polym. Technol. Appl.* 2 (2021) 100079.
- [32] P. Negrea, A. Caunii, I. Sarac, M. Butnariu, The study of infrared spectrum of chitin and chitosan extract as potential sources of biomass, *Dig. J. Nanomater. Bios.* 10 (4) (2015) 1129–1138.
- [33] Z. Yin, R. Chu, L. Zhu, S. Li, F. Mo, D. Hu, C. Liu, Application of chitosan-based flocculants to harvest microalgal biomass for biofuel production: a review, *Renew. Sust. Energ. Rev.* 145 (2021) 111159.
- [34] S.S. Vedula, G.D. Yadav, Chitosan-based membranes preparation and applications: challenges and opportunities, *J. Indian Chem. Soc.* 98 (2021) 100017.
- [35] A. Primo, F. Quignard, Chitosan as efficient porous support for dispersion of highly active gold nanoparticles: design of hybrid catalyst for carbon-carbon bond formation, *Chem. Commun.* 46 (2010) 5593–5595.
- [36] K.D. Trimukhe, A.J. Varma, Metal complexes of crosslinked chitosans: correlations between metal ion complexation values and thermal properties, *Carbohydr. Polym.* 75 (2009) 63–70.
- [37] M. Kaloti, H.B. Bohidar, Kinetics of coacervation transition versus nanoparticle formation in chitosan-sodium tripolyphosphate solutions, *Colloids Surf. B* 81 (1) (2010) 165–173.
- [38] H. Karimi-Maleh, A. Ayati, R. Davoodi, B. Tanhaei, F. Karimi, S. Malekmohammadi, Y. Orooji, L. Fu, M. Sillanpää, Recent advances in using of chitosan-based adsorbents for removal of pharmaceutical contaminants: a review, *J. Clean. Prod.* 291 (2021) 125880.
- [39] A.R. Modarresi-Alam, M. Nasrollahzadeh, M. Sajjadi, H.A. Khonakdar, Synthesis of 5-arylamino-1*H* (2*H*)-tetrazoles and 5-amino-1-aryl-1*H*-tetrazoles from secondary arylcyanamides in glacial acetic acid: a simple and efficient method, *Turk. J. Chem.* 33 (2) (2009) 267–280.
- [40] M. Nasrollahzadeh, Z. Issaabadi, R.S. Varma, Magnetic lignosulfonate-supported Pd complex: renewable resource-derived catalyst for aqueous Suzuki-Miyaura reaction, *ACS Omega* 4 (10) (2019) 14234–14241.
- [41] G. Aromí, L.A. Barrios, O. Roubeau, P. Gamez, Triazoles and tetrazoles: prime ligands to generate remarkable coordination materials, *Coord. Chem. Rev.* 255 (2011) 485–546.
- [42] P.N. Gaponik, S.V. Voitekhovich, A.S. Lyakhov, V.E. Matulis, O.A. Ivashkevich, M. Quesada, J. Reedijk, Crystal structure and physical properties of the new 2D polymeric compound bis(1,5-diaminotetrazole)dichlorocupper(II), *Inorg. Chim. Acta* 358 (2005) 2549–2557.
- [43] M. Muttenthaler, M. Bartel, P. Weinberger, G. Hilscher, W. Linert, Synthesis and characterisation of new ditetrazole-ligands as more rigid building blocks of envisaged iron(II) spin-crossover coordination polymers, *J. Mol. Struct.* 741 (2005) 159–169.
- [44] A. Bialońska, R. Bronisz, M. Weselski, A new family of spin-crossover complexes based on a Fe^{II}(Tetrazolyl)₄(MeCN)₂-type core, *Inorg. Chem.* 47 (2008) 4436–4438.
- [45] Popova E.A., N.A. Bokach, M. Haukka, R.E. Trifonov, V.A. Ostrovskii, A new route to N(1)-5R-tetrazole complexes via azidation to nitriles coordinated to Pt(II) and Pt(IV), *Inorg. Chim. Acta* 375 (2011) 242–247.
- [46] M. Liu, X. Guo, L. Hu, H. Yuan, G. Wang, B. Dai, L. Zhang, F. Yu, $\text{Fe}_3\text{O}_4/\text{Fe}_3\text{C}$ @nitrogen-doped carbon for enhancing oxygen reduction reaction, *ChemNanoMat* 5 (2) (2019) 187–193.